ISSN 1330-3651 (Print), ISSN 1848-6339 (Online)
https://doi.org/10.17559/TV-20250414002593
Original scientific paper

Winding Materials Effect on Performance of Air Core Current Limiting Reactors in Energy Systems

Murat AYAZ*, Cüneyt CEYHAN, Kadir YILMAZ, Yiğit KARABULUT

Abstract: The rapid increase in energy demand requires expanding the capacities of energy transmission and distribution systems, which in turn raises fault current magnitudes and risks damaging existing switchgear. To address this, current-limiting reactors (CLRs) are used to control these fault currents. This study presents the development of an air-core reactor design with copper windings and evaluates the performance of a similar reactor with aluminium windings under equivalent cross-sectional and resistance conditions. Preliminary dimensions for the reactor were determined using analytical methods for a 5-10 A, 5 V AC, 50 Hz system. A 1/10000 scale model of the CLR was created using Ansys Maxwell software. Based on the design and performance analysis, prototypes with both copper and aluminium windings were produced. The winding loss analysis was performed, and temperature distributions were assessed for both pre- and post-short-circuit conditions. The simulations were conducted under varying current magnitudes and harmonic distortions to assess frequency-dependent behaviour. During testing, a system drawing of approximately 4.9 A rms at 4.9 V rms was limited to 3.5 A rms when the copper-wound CLR was activated. The CLR effectively reduced the current by about 28%, with experimental results showing similar performance for both aluminium and copper-wound CLRs. The study also included a comparison of aluminium and copper-wound CLRs regarding cost, volume, and weight, highlighting the trade-offs between material choices.

Keywords: air core reactor; aluminium conductor; copper conductor; current limiting reactor; energy systems; winding materials

1 INTRODUCTION

Energy is delivered to the end user through generation, transmission, and distribution systems. In recent years, the rapidly increasing energy demand has necessitated the expansion of these systems' capacities. As capacities increase, the power flow within facilities also rises, leading to higher magnitudes of fault currents, which can cause significant damage to existing switchgear [1-5]. Fault currents in power systems can reach up to 20 times the nominal current [6], making the management of short-circuit currents a critical factor in determining the size and cost of power equipment such as circuit breakers, busbars, transmission lines, and transformers [7].

Given these challenges, research on alternative methods to effectively reduce short-circuit currents has intensified. Current-limiting reactors (CLR) and fault current limiters (FCL) are commonly used equipment-based methods to mitigate fault currents [8-10, 11-16]. In air-core CLRs, the use of air as the magnetic core prevents magnetic saturation, even as current magnitude increases. This ensures that the inductance value remains constant, avoiding sudden inductance changes in the system. However, the structural characteristics of air-core reactors can lead to heat generation due to alternating current losses and eddy current losses. To manage this, air ducts are integrated between windings to facilitate effective cooling. Additionally, protective structures must be examined to ensure they do not hinder the reactor's cooling process [17-19].

Recent advancements in current-limiting technologies have led to numerous studies focusing on the design, optimization, and implementation of CLRs in both AC and DC power systems. Several works have addressed parameter optimization and configuration of CLRs in DC microgrids and HVDC systems [20, 21], as well as dynamic temperature rise monitoring through digital twin models [22]. The impact of CLRs on bulk power networks has been demonstrated through practical case studies [23], while others have investigated their integration into multi-terminal HVDC systems and modular multilevel converters [24, 25]. In addition, auxiliary winding systems for managing inrush currents in shunt reactors have been explored [26]. Electromagnetic modelling approaches for air-core reactors used in solid-state fault current limiters have also been presented [27]. The role of CLRs in enhancing protection strategies for DC networks has been emphasized through energy-based and differential protection techniques [28, 29]. These studies collectively underscore the importance of CLRs in improving reliability, efficiency, and protection of modern power systems.

Mechanical strength is another crucial design criterion for air-core reactors. Series-connected current-limiting reactors must withstand mechanical deformations caused by short-circuit currents. The finite element analysis method helps determine the forces resulting from these currents and assess safety factors to predict potential deformations [30]. Noise levels, which can arise from mechanical forces generated by electromagnetic fields, must also be managed, with international standards requiring sound levels to be below 85 dB [31].

In addition to these traditional methods, non-superconducting fault current limiters (NSFCL) have emerged as cost-effective alternatives to superconducting fault current limiters (SFCL). NSFCLs offer advantages such as extended equipment life, reduced power losses, and enhanced system stability at a lower cost compared to SFCLs [32-35]. These benefits make NSFCLs an attractive option for managing fault currents in power systems.

Similarly, the choice of materials used in electrical machines, such as copper and aluminium windings, is an important consideration. Copper windings have traditionally been used to create magnetic fields due to their superior performance. However, aluminium is increasingly being explored as a viable alternative due to its lower density and cost advantages. Studies indicate that while aluminium windings are lighter and more cost-effective than copper, they may lead to a slight reduction in efficiency and require additional cooling [36, 37]. These

findings are consistent with observations in other applications like induction motors and distribution transformers, where aluminium windings, though comparable in efficiency to copper, may necessitate design modifications [38-40].

Although the literature includes a wide range of studies on current-limiting reactors (CLRs), many of these works primarily focus on system-level simulation, specific topological configurations, or thermal modelling without offering comprehensive experimental validation. For instance, some studies investigate parameter selection for DC microgrids [20], optimization in HVDC transmission systems [21, 24], or digital twin models for temperature estimation [22], while others concentrate on electromagnetic modelling through FEM [19, 27] or general thermal behaviour [11]. However, most lack material-focused evaluations or real-world experimental implementation. In contrast, the present study not only introduces a validated air-core CLR prototype using both copper and aluminium windings under equal electrical design conditions, but also incorporates cost analysis, temperature rise evaluation, and efficiency comparison. Tab. 1 summarizes the technical focus and scope of selected prior studies compared to the comprehensive performance-based assessment conducted in this work.

Table 1 Comparative overview of CLR-focused studies

Study/Reference	System Type	Simulation	Experimental	Material Evaluation	Thermal Analysis	Cost Analysis	Contribution
[11] Nurminen	Air-core CLR	✔	✘	✘	✔	✘	Thermal modeling of dry-type CLR
[19] Yuan et al.	Air-core CLR	✔	✘	✘	✔	✘	FEM-based thermal optimization
[20] Huang et al.	DC microgrid CLR	✔	✘	✘	✘	✘	Parameter design for DC systems
[21] Zhu & Li	HVDC CLR	✔	✘	✘	✘	✘	LCC-MMC based optimization
[22] Zhou et al.	Air-core CLR	✔	✘	✘	✔	✘	Digital twin for dynamic heating
[23] Shah	Bulk power CLR	✔	✘	✘	✘	✘	System-level case study impact
[24] Xing et al.	HVDC CLR	✔	✘	✘	✘	✘	Topology config for multi-terminal HVDC
[27] Akin et al.	SPRFCL Series Inductor	✔	✘	✘	✘	✘	2D FEM for electromagnetic modeling
The proposed study	Air-core CLR	✔	✔	✔	✔	✔	Full experimental and analytical Cu-Al material comparison under equal design conditions

This study presents detailed insights into the effective use of current-limiting reactors (CLRs) in energy transmission and distribution systems. A copper-wound air-core reactor was designed, and an equivalent aluminium-wound version was developed under matched cross-sectional and resistance conditions. Following analytical design and simulation, both prototypes were manufactured and experimentally tested under short-circuit conditions. Winding loss analyses and thermal evaluations were conducted for both pre-fault and post-fault states. Simulations were also performed at 50%, 100%, and 150% of the nominal operating current to assess electromagnetic behaviour under varying load conditions. Additionally, a 250 Hz component representing the 5th harmonic (at 10% amplitude of the fundamental) was applied to evaluate harmonic sensitivity. The study further compares the two winding materials in terms of electrical performance, weight, volume, and cost, offering a balanced perspective on performance versus economic feasibility in practical CLR applications.

2 AIR-CORE REACTOR DESIGN

In this study, a system with a peak fault current of 50 kA/s (I_{kp}) was designed to limit the short-circuit current to 40 kA/s (I_{kn}). Due to the difficulty and high cost of creating a reactor for a real system, a scaled-down model at 1/10000 scale was used. This approach, which follows the electromagnetic similarity principle, is widely used to enable practical laboratory evaluation of full-scale reactor behaviour. Similar scaled modelling strategies have been validated in the literature for analysing magnetic field distribution, thermal characteristics, and fault behaviour in air-core reactors [40-45]. After designing, analysing, and optimizing the required reactor, prototypes were produced accordingly. The reactor design and production were examined with different winding materials, including copper and aluminium, under equal cross-sectional and resistance conditions. Performance data for these materials were evaluated, and the proposed reactor specifications are listed in Tab. 2.

For prototype testing, the system voltage was set at 5 V AC, and the nominal current was 1 A. Fault currents were scaled down to I_{kp}: 5A/s and I_{kn}: 4A/s. The required impedance for the current-limiting reactor (CLR) to limit the fault current from 5 A/s to 4 A/s was calculated using Eq. (1):

$$XL_{kp} = \frac{V}{I_{kp}} \tag{1}$$

Here, XL_{kp} represents the system impedance without the current-limiting reactor. The target short-circuit current is I_{kn}: 4 A/s. The system impedance can be determined using Eq. (2):

$$XL_{kn} = \frac{V}{I_{kn}} \tag{2}$$

With the reactor in place, the system impedance should be 1.25 ohms to reduce the fault current to the desired level. To achieve this, a series impedance of 0.25 ohms needs to

be added to the system, increasing the impedance from 1 ohm to 1.25 ohms. The CLR inductance value corresponding to the impedance calculated with Equation 3 is:

$$L = \frac{XL}{2\pi f} \tag{3}$$

Table 2 The proposed reactor specifications

Description	Value	Unit	Abbreviation
Voltage	5	VAC	V
Frequency	50	Hz	f
Peak fault current	5	A	I_{kp}
Nominal fault current	4	A	I_{kn}
Current limiting percentage	20	%	CR
Nominal current	1	A	In
Conductor diameter	1	mm	D
Temperature class	F - 155	°C	-
Permeability of air	$4\pi\ 10^{-7}$	-	μ_0
Inductance value	0.79	mH	L
Impedance value	0.25	Ω	XL
Voltage drops	4	%	-
Recovery time	1	s	-
Reactor inner diameter	28	cm	-
Standard	IEC 60076-6		
Conductor type	Enamel-coated Cu & Al		

Once the inductance value is determined, the specifications for conductors used in the reactor for a 5 V AC system are identified. The conductor cross-section is chosen based on continuous current and short-term temporary current values. For continuous current, the maximum current density is 2 A/mm² for copper conductors and 1.2 A/mm² for aluminium conductors. For a continuous current of 1 A, the minimum cross-section for aluminium conductors is 0.8 mm², and for copper conductors, it is 0.5 mm². The outer diameter of the conductors, without insulation, should be at least 1.0 mm for aluminium and 0.8 mm for copper.

According to IEC 60076-5, the temperature after short-term fault currents is calculated using Eqs. (4) and (5) for aluminium and copper windings, respectively:

$$\theta_1 = \theta_0 + \frac{2(\theta_0 + 225)}{\frac{45700}{J^2 t} - 1} \tag{4}$$

$$\theta_1 = \theta_0 + \frac{2x(\theta_0 + 235)}{\frac{106000}{J^2 t} - 1} \tag{5}$$

Here, θ_0 is the initial wire temperature (25 °C), and t is the short-circuit duration (1 s). For dry-type transformers with an insulation temperature class of 155 °C (Class F), the maximum allowable temperature values differ based on the conductor material. Specifically, the copper-wound transformer can reach up to 350 °C, whereas the aluminium-wound transformer has a lower maximum temperature limit of 200 °C.

For aluminium windings, the maximum allowable temperature is 200 °C, and for copper windings, it is 350 °C, assuming an ambient temperature of 25 °C. The reactor temperature after a short-circuit can be verified against these limits using Eqs. (4) and (5) for the respective conductor cross-sections. The calculations show that a short-term short-circuit current causes a temperature rise of 0.44 °C in aluminium windings and 0.2 °C in copper windings. Considering the ambient temperature, these temperature increases remain within the allowable limits, confirming the suitability of the selected conductor cross-sections.

These temperature increases comply with the IEC 60076-5 standard for thermal class "F". Given the 1/10000 scaling of the short-circuit value, the required cross-sectional area can be approximately calculated for the real system. The reactor design specifies a minimum conductor outer diameter of 1 mm for both materials. The number of turns required, based on the inductance value, is calculated using Eq. (6), and the optimal number of turns is determined using finite element analysis.

$$L = \mu_0 \frac{\pi r^2 N^2}{h + 0.9r} \tag{6}$$

Voltage drop percentage and current limiting percentage are calculated using Eqs. (7) and (8), respectively, with a current limiting percentage of 20% obtained for the proposed system.

$$V = \frac{Vk_p - Vk_n}{Vk_p} \tag{7}$$

$$CR = \frac{Ik_p - Ik_n}{Ik_p} \tag{8}$$

The 3D model and basic dimensions of the current-limiting reactor are shown in Fig. 1.

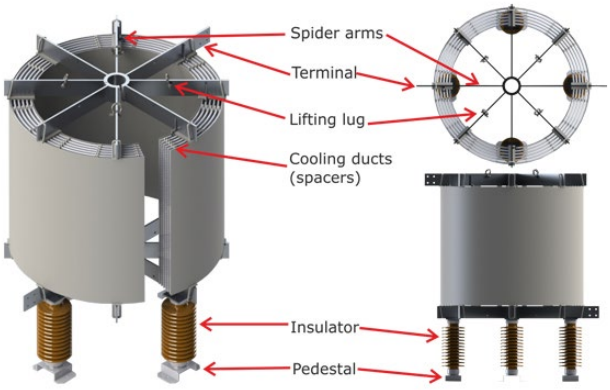

Figure 1 Model of an air-core current-limiting reactor [46]

3 SIMULATION STUDY AND RESULTS

The electromagnetic analysis of the CLR, with its fundamental dimensions determined, was conducted to optimize the design using a 3D model created in Ansys Maxwell software. The 3D model of the proposed CLR is shown in Fig. 2. The model was constructed using geometric symmetry, and the materials were assigned based on nonlinear BH curves provided in the manufacturer's datasheets. The electromagnetic solution

domain was defined to capture the reactor's performance under both static and transient conditions.

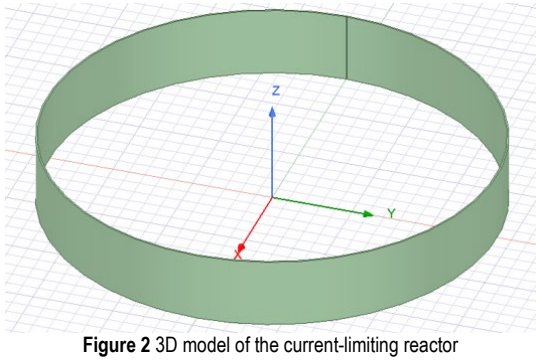

Figure 2 3D model of the current-limiting reactor

To ensure numerical accuracy and convergence, mesh generation was performed using Ansys Maxwell's advanced adaptive meshing algorithm. A total of 12,633 triangular elements were generated. In regions with high field intensity such as air gaps and conductor edges local mesh refinement was applied with a minimum edge length of 3.58 µm. The mesh was divided into two primary regions: PolygonNek1_Separate1 (4330 elements) and Region (8303 elements). The RMS edge lengths of these zones were calculated as 0.0001278 m and 0.0177 m, respectively. Additionally, the standard deviation of element areas was approximately 0.00045 m², indicating uniform mesh distribution and ensuring the stability of the numerical solution.

To further enhance the accuracy of the magnetic field distribution, the solution domain in Ansys Maxwell was extended beyond the physical boundaries of the reactor using the CreateRegion command. In air-core reactors, overly narrow solution domains may truncate the natural spread of magnetic flux, leading to artificial field confinement and significant computational errors. To mitigate this, the outer region was defined using the Percentage Offset method expanded by 1000% along the *X*-axis and by 10% along both the *Y* and *Z* axes. Additionally, to simulate the natural decay of the magnetic field at far distances, a Balloon boundary condition was applied to the outermost surfaces. This approach ensured that the boundary would not artificially distort the field, thereby improving the reliability of the simulation results, especially under high magnetic flux conditions.

Following the geometric and meshing definitions described above, the simulation was executed using the Transient solver in Ansys Maxwell. The total simulation time was defined as 100 ms with a time step of 1 ms. To maintain numerical stability, the nonlinear residual tolerance was set to 1×10^{-4}. The solution method was configured in General Transient mode, and time decomposition parameters were adjusted accordingly to accurately capture the reactor's dynamic behaviour.

Optimization was performed through parametric analyses, focusing on variables such as the number of turns, reactor diameter, conductor length, and inductance. Fig. 3a illustrates the change in inductance as a function of radius obtained from the parametric analysis. The number of turns was varied between 20 and 40, while the radius was adjusted within the range of 40 mm to 150 mm. Similarly, Fig. 3b depicts the conductor length obtained for various numbers of turns as a function of the radius. Although it is possible to achieve the previously calculated inductance with different radii and turn values, a radius of 140 mm and 40 turns were selected for this study.

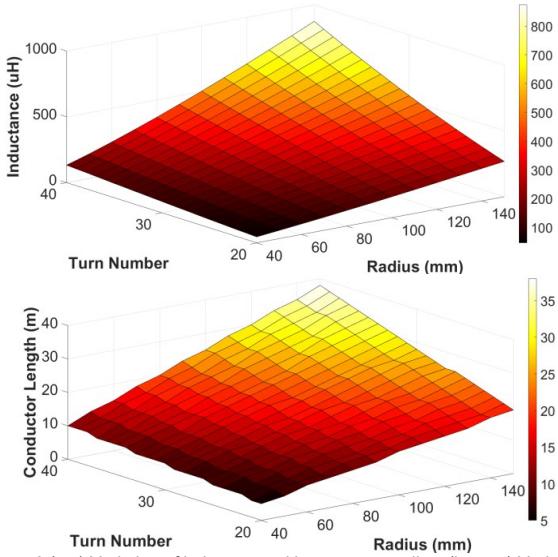

Figure 3 (top) Variation of inductance with respect to radius; (bottom) Variation of conductor length with respect to radius

After determining the necessary number of turns, optimal inner diameter, and height using the Ansys Maxwell Magnetostatic solver, the transient behaviour of the reactor under short-circuit conditions was analysed with the Ansys Maxwell Transient solver. The excitation circuit of the system was designed, as shown in Fig. 4, to test the short-circuit condition. Initially, the system was subjected to fault current without the reactor. In the second scenario, the current-limiting reactor was integrated, and the change in current amplitude was analysed.

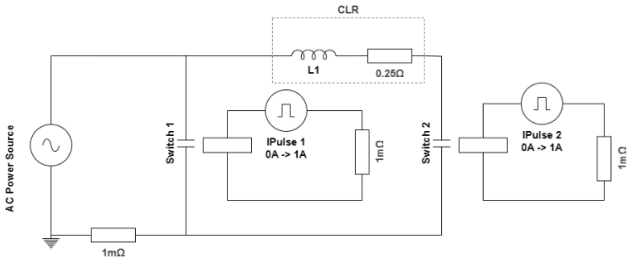

Figure 4 Configuration of the excitation circuit for current-limiting reactor testing

As illustrated in Fig. 5, the scaled-down reactor was tested under three operating conditions, with the current-limiting reactor engaged at 25 ms. In the reduced load scenario, the peak fault current decreased from 3.53 A to 2.67 A, corresponding to a 24.4% reduction. Under nominal load with harmonic injection, the fundamental peak was limited from 7.06 A to 5.35 A (24.2%), while the 250 Hz harmonic component decreased from 0.71 A to 0.39 A, reflecting a 45.1% suppression. Corresponding RMS values also decreased from approximately 4.99 A to 3.78 A, confirming a 24.2% reduction in effective current amplitude. At the overload level of $1.5 \times I_n$, the current was reduced from 10.60 A to 8.02 A, indicating a 24.3% limitation. In all operating scenarios, the inductance value remained stable at 0.79 mH, as shown in the simulation results. This confirms that the air-core structure does not undergo magnetic saturation, ensuring consistent dynamic behaviour regardless of current level.

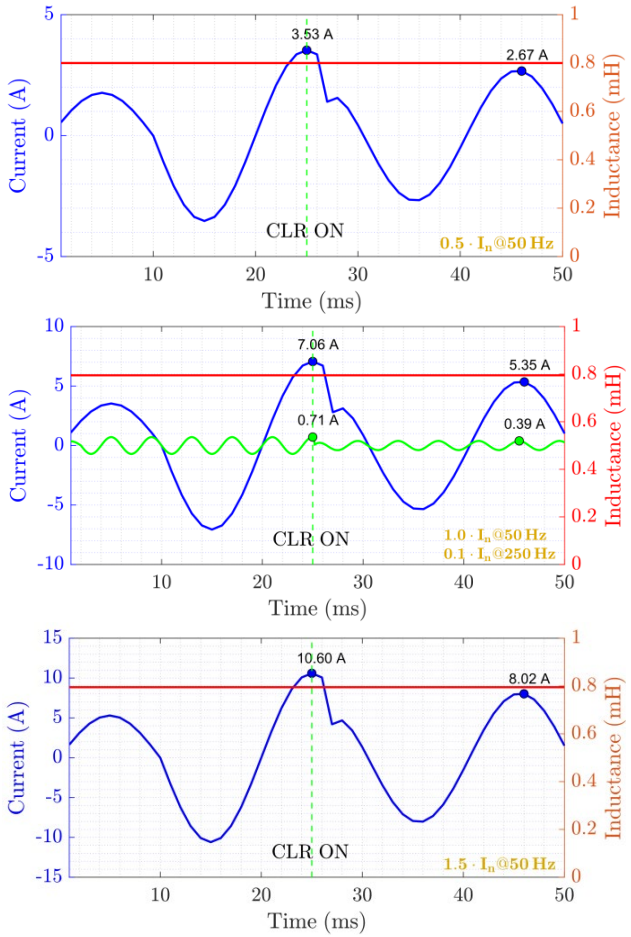

Figure 5 Current-limiting performance of the scaled-down prototype reactor

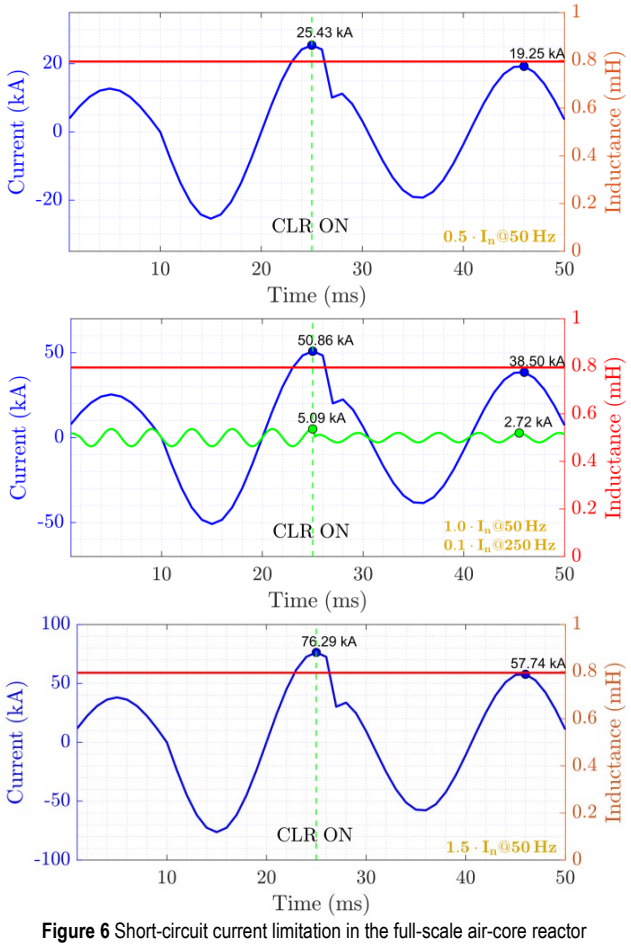

Figure 6 Short-circuit current limitation in the full-scale air-core reactor

The full-scale air-core CLR model, shown in Fig. 6, exhibits similar limiting behaviour under scaled-up system conditions. At half load, the peak current was reduced from 25.43 kA to 19.25 kA, a 24.3% decrease. In the nominal load with harmonic case, the peak dropped from 50.86 kA to 38.50 kA (24.3%), while the 250 Hz harmonic was suppressed from 5.09 kA to 2.73 kA, yielding a 46.3% attenuation. Under overload, a similar reduction from 76.29 kA to 57.74 kA (24.3%) was observed.

Fig. 7 presents the results for the iron-core reactor under identical test scenarios. Peak current reductions were again consistent: 25.43 kA to 19.25 kA at 0.5 × *In*, and 76.29 kA to 57.74 kA at 1.5 × *In*, both reflecting a 24.3% reduction. The 250 Hz harmonic component decreased from 5.09 kA to 2.77 kA, corresponding to a 45.6% suppression. Notably, a change in inductance was observed under high fault conditions: the initial inductance of 1 mH gradually decreased to approximately 0.8 mH, indicating the onset of magnetic core saturation.

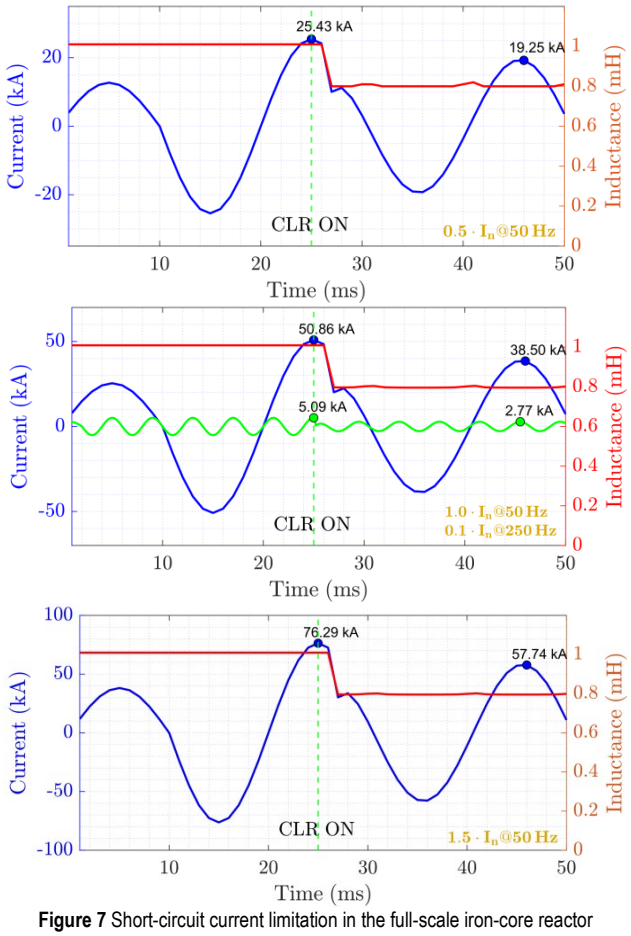

Figure 7 Short-circuit current limitation in the full-scale iron-core reactor

These results indicate that if the ASR had been designed with an iron core, as shown in Fig. 7, the inductance would collapse, causing the iron core to behave like an air-core reactor. Consequently, the system would not generate the desired reactance, leading to undesirable faults and disadvantages in the system.

In addition to calculating the inductance value, time-dependent analyses of the reactor also assessed the associated ohmic (stranded) losses. When the reactor was activated at the 25th millisecond, the average winding losses under nominal loading were found to be 14.13 W for copper and 22.0 W for aluminium. The time-dependent

evolution of these losses is depicted in Fig. 8, highlighting the differences in loss dynamics between the two conductor types at the rated current level.

To extend this comparison across a wider operating range, further simulations were performed at 0.5 × *In* and 1.5 × *In*. For copper, RMS losses increased from 3.04 W at 0.5 × *In* to 27.66 W at 1.5 × *In*. Aluminium showed a similar trend, with losses ranging from 4.65 W to 37.20 W. Although copper typically exhibited lower overall losses, aluminium consistently produced higher maximum loss values, indicating a greater likelihood of localized thermal stress under elevated current conditions.

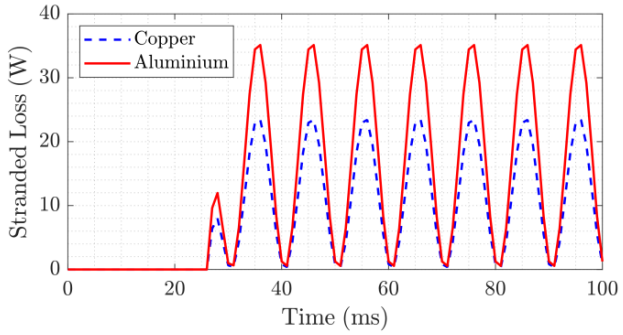

Figure 8 Stranded loss comparison in copper and aluminium-wound reactors

A thermal analysis conducted based on the calculated 22 W loss in the reactor revealed a temperature increase of 0.18 °C. Fig. 9 shows the temperature distribution resulting from the thermal analysis, indicating that the temperature difference on the reactor aligns with the analytically calculated value.

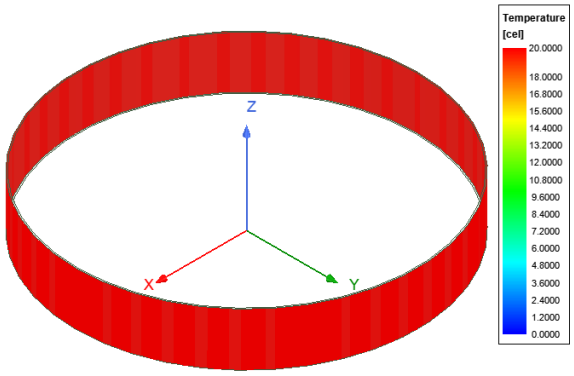

Figure 9 Temperature analysis of the current-limiting reactor

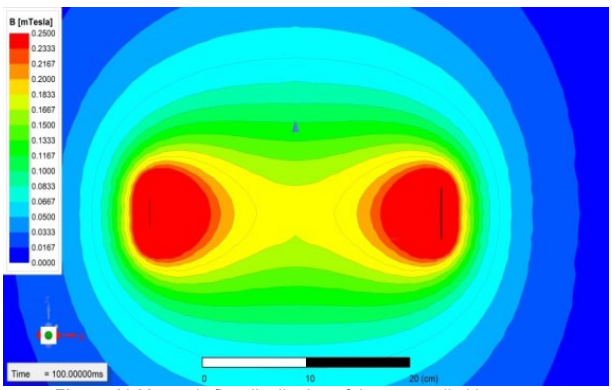

Figure 10 Magnetic flux distribution of the current-limiting reactor

Air-core current-limiting reactors possess free magnetic fields, necessitating careful calculations regarding their impact on human health following installation. The threshold for magnetic field exposure should not exceed 0.2 mT in general residential areas, while up to 1.0 mT is permissible in work environments. The magnetic flux density distribution of the designed reactor, shown in Fig. 10, indicates a flux density of 0.233 mT at the reactor's zero point, which rapidly decreases to zero over a short distance.

4 EXPERIMENTAL TESTS AND DISCUSSION

To validate the design parameters of the current-limiting reactor, prototypes were produced. Two separate prototypes of the CLR were manufactured using copper and aluminium winding materials. For a fair comparison, both CLR prototypes were designed and produced with identical electrical properties. The experimental test setup for testing the current-limiting application of the reactors is shown in Fig. 11. All equipment in the test setup was numbered, and their details are provided in Tab. 3.

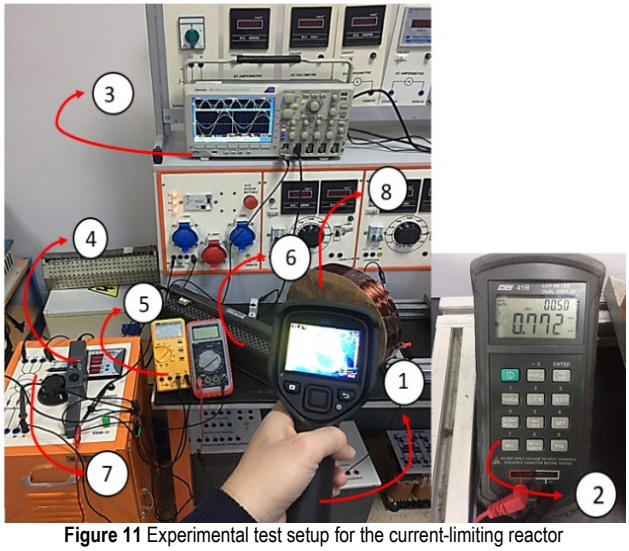

Figure 11 Experimental test setup for the current-limiting reactor

Table 3 Test setup equipment and specifications

No	Description	Brand	Model
1	Thermal camera	FLIR	FLIR-E6390
2	LCR meter	CHY	CHY 41R
3	Oscilloscope	TEKTRONIX	DPO 3054
4	Current probe	FLUKE	10 mV/A
5	Multimeter	CLASS	MY62
6	Rheostat	PHYWE	8 A, 10 Ohm
7	Variac	-	3 Phase
8	CLR	-	Air-core

4.1 Tests on Copper-Wound CLR

Experimental tests were conducted separately for both reactors under identical conditions. First, the inductance of the copper-wound CLR was measured using an LCR meter, yielding an inductance value of 0.758 mH. Considering that the analytical and simulation studies indicated an inductance value of 0.790 mH, the experimental measurement confirmed the design.

In a system drawing approximately 4.9 A rms current at 4.9 V rms, the activation of the copper-wound CLR reduced the current from 4.9 A rms to 3.5 A rms. The short-circuit event and current variation were recorded using an

oscilloscope, as shown in Fig. 12. It was observed that the CLR limited the current by approximately 28%.

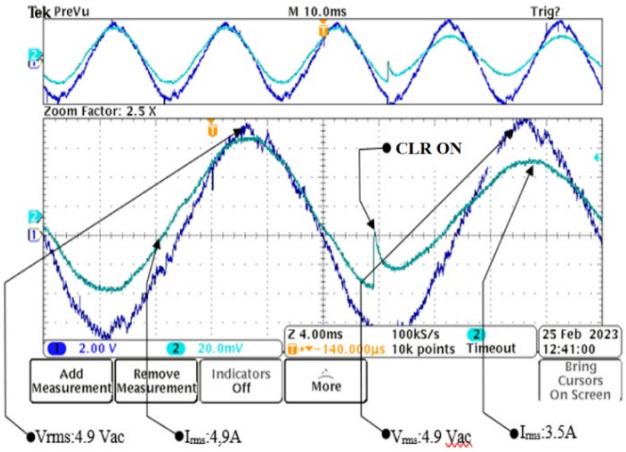

Figure 12 Short-circuit behaviour of copper-wound current-limiting reactor

Thermal measurements before and after the test were conducted on the copper-wound CLR using a FLIR thermal camera. The camera's emissivity was set to 0.95, and images were captured from approximately 1 meter, as shown in Fig. 13. The ambient temperature was 24.4 °C, and the CLR was at the same temperature before the short-circuit test. After one second of short-circuit current flow, the temperature increased by 0.3 °C to 24.7 °C. This temperature rise does not adversely affect the reactor's performance.

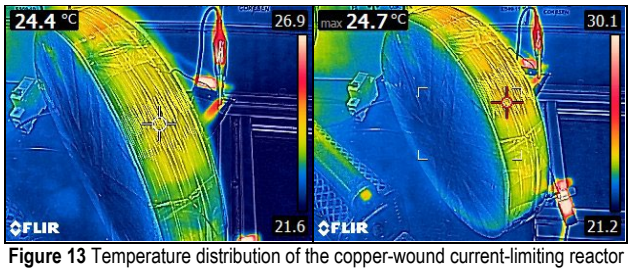

Figure 13 Temperature distribution of the copper-wound current-limiting reactor (CLR) before (left) and after (right) the short-circuit event

4.2 Tests on Aluminium-Wound CLR

The aluminium-wound CLR was designed and manufactured to have the same electrical properties as the copper-wound reactor. The inductance of the aluminium-wound CLR, produced with the same diameter and number of turns as the copper-wound CLR, was measured at 0.736 mH. This value is slightly lower than the copper-wound CLR, potentially due to less compact winding resulting from the use of double wires and associated workmanship factors.

As with the copper-wound CLR tests, in a system drawing approximately 4.9 A rms current at 4.9 V rms, the aluminium-wound CLR reduced the current from 4.9 A rms to 3.5 A rms upon activation. The short-circuit event and current variation were recorded using an oscilloscope, as shown in Fig. 14. It was observed that the CLR limited the current by approximately 28%. The results demonstrated that the experimental performances of the aluminium and copper-wound CLRs were comparable.

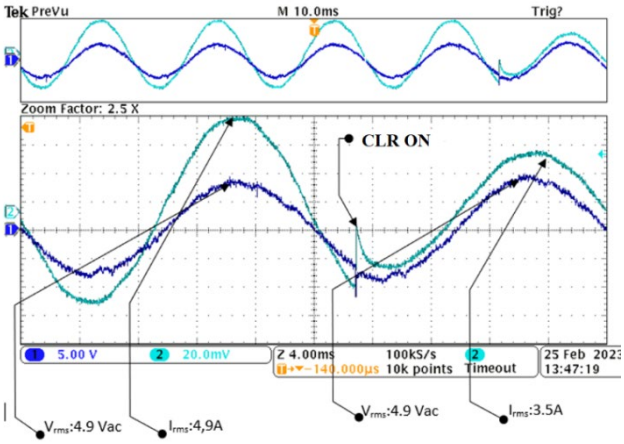

Figure 14 Short-circuit behaviour of alluminium-wound current-limiting reactor

Thermal measurements before and after the test were conducted on the aluminium-wound CLR using a FLIR thermal camera. The camera's emissivity was set to 0.95, and images were captured from approximately 1 meter, as shown in Fig. 15. Before the short-circuit test, the temperature of the CLR was 22.0 °C. After one second of short-circuit current flow, the temperature increased by 0.5 °C to 22.5 °C. This temperature rise does not adversely affect the reactor's performance.

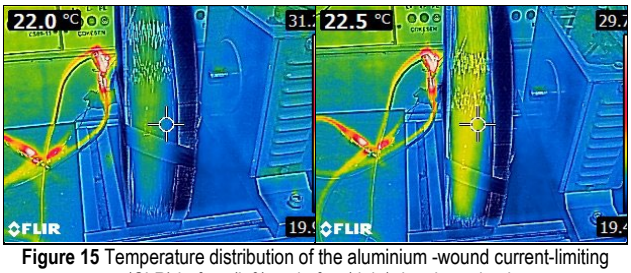

Figure 15 Temperature distribution of the aluminium -wound current-limiting reactor (CLR) before (left) and after (right) the short-circuit event

4.3 Comparison of Copper and Aluminium-Wound Reactors

Current-limiting reactors are systems that can operate for many years without requiring maintenance. Therefore, designing cost-effective reactors during the initial installation phase is crucial. However, since these reactors remain in operation continuously, energy losses must also be considered as part of operating costs, emphasizing the importance of achieving high efficiency.

This study examined the advantages and disadvantages of using copper and aluminium as winding materials in air-core CLRs. While the experimental tests evaluated equivalent resistance, this section provides a detailed comparison based on equivalent resistance and cross-sectional area for both materials.

In both reactor designs, the coil diameter and number of turns were kept constant, resulting in identical conductor lengths. Under these conditions, resistance values for the winding materials can be calculated using Eq. (9), where ρ is the material's resistivity, l is the conductor length, and S is the cross-sectional area. Using Eq. (10), the winding mass is calculated based on material density. Similarly, for reactors with equivalent resistance, conductor cross-sectional areas and diameters are determined using Eq. (11). The calculated parameters for scaled-down CLRs are

shown in Tab. 4. Average market prices were used for cost analysis: $8700 USD/ton for copper and $2535 USD/ton for aluminium [47].

$$R_{\mathrm{cu}} = \rho_{\mathrm{cu}} \frac{l}{S_{\mathrm{cu}}} R_{\mathrm{Al}} = \rho_{\mathrm{Al}} \frac{l}{S_{\mathrm{Al}}} \tag{9}$$

$$m_{\mathrm{cu}} = \gamma_{\mathrm{cu}} l S_{\mathrm{cu}} m_{\mathrm{Al}} = \gamma_{\mathrm{Al}} l S_{\mathrm{Al}} \tag{10}$$

$$R_{\mathrm{cu}} = R_{\mathrm{Al}} \rightarrow \frac{\rho_{\mathrm{cu}}}{S_{\mathrm{cu}}} = \frac{\rho_{\mathrm{Al}}}{S_{\mathrm{Al}}} \rightarrow S_{\mathrm{Al}} = S_{\mathrm{cu}} \frac{\rho_{\mathrm{Al}}}{\rho_{\mathrm{cu}}} \tag{11}$$

Table 4 Comparison of copper and aluminium-wound reactor designs

Parameter	Copper	Equivalent Cross-Section: Aluminium	Equivalent Resistance: Aluminium
D / mm	1	1	1.294
S / mm^2	0.785	0.785	1.318
R / Ω	0.0756	0.127	0.0756
m / g	248.8	74.0	125.78
Cost / USD	2.17	0.20	0.33

Aluminium wires, being lighter than copper, offer advantages in reactor design. While aluminium is 70% lighter than copper at equivalent cross-sections, its 68% higher resistance may increase energy losses, negatively affecting long-term operational costs. Nevertheless, aluminium is 91% more economical than copper in terms of material cost. For equivalent resistance, aluminium's cross-sectional area must increase by 68%. This increase expands the wire diameter by 29.4%, while the weight remains 50% lower than copper, offering a significant advantage. However, a larger diameter can increase the size and cost of mechanical components, such as support rods and surface protectors, needed to maintain coil shape. Despite requiring larger cross-sections to match energy losses, aluminium remains 85% more economical than copper, making it an attractive alternative in cost-sensitive applications. These findings highlight the critical need to balance electrical and mechanical properties in reactor design.

5 CONCLUSION

This study has thoroughly examined the design, prototyping, and performance evaluation of air-core current-limiting reactors, aiming to manage short-circuit currents in energy transmission and distribution systems. The comparative analysis of copper and aluminium windings, supported by experimental and simulation data, has revealed critical insights into the performance, cost, and practicality of these materials under equivalent design conditions. The findings confirmed that air-core reactors effectively limited short-circuit currents by 28%, significantly reducing the stress on protective devices and contributing to the overall reliability and safety of power systems.

Copper windings demonstrated clear advantages in terms of energy efficiency, offering 36% lower resistance and reduced energy losses compared to aluminium. These properties make copper an ideal choice for applications prioritizing high performance and minimal operational losses. Conversely, aluminium windings emerged as a highly economical alternative, being 50% lighter and 85% more cost-effective than copper, highlighting their potential for cost-sensitive applications. Despite these material differences, both prototypes adhered to international standards regarding temperature rise under short-circuit conditions, demonstrating their suitability for practical implementation. Moreover, the thermal and electromagnetic analyses revealed that both materials maintained consistent inductance values and thermal stability during fault conditions, ensuring reliable operation without significant performance degradation. While copper remains the preferred option for maximizing energy efficiency, aluminium presents a viable option for reducing initial installation costs and overall system weight, albeit with careful consideration of design modifications to address its higher resistance.

The results of this study underscore the versatility and importance of air-core reactors in modern energy systems, providing not only a reliable means to manage fault currents but also an adaptable platform for optimizing material selection based on specific technical and economic constraints. This work offers a comprehensive framework for balancing performance and cost in reactor designs, serving as a valuable reference for future research and industrial applications.

6 REFERENCES

[1] Chewale, M., Savakhande, V., Jadhav, R., Kupwade, R., & Siddha, P. (2019, March). A comprehensive review on fault current limiter for power network. *2019 International Conference on Recent Advances in Energy-efficient Computing and Communication (ICRAECC)*. https://doi.org/10.1109/ICRAECC43874.2019.8995098

[2] Alam, M. S., Abido, M. A. Y., & El-Amin, I. (2018). Fault current limiters in power systems: A comprehensive review. *Energies*, *11*(5), 1025. https://doi.org/10.3390/en11051025

[3] Patil, S. & Thorat, A. (2017, February). Development of fault current limiters: A review. *2017 International Conference on Data Management, Analytics and Innovation (ICDMAI).* https://doi.org/10.1109/ICDMAI.2017.8073496

[4] Yadav, S., Choudhary, G. K., & Mandal, R. K. (2014). Review on fault current limiters. *International Journal of Engineering Research & Technology (IJERT)*, *3*(4), 1595-1603.

[5] Schmitt, H. (2006, June). Fault current limiters report on the activities of CIGRE WG A3. 16. *2006 IEEE Power Engineering Society General Meeting.* https://doi.org/10.1109/PES.2006.1709205

[6] Seyedi, H. & Tabei, B. (2012). Appropriate placement of fault current limiting reactors in different HV substation arrangements. *Circuits and Systems*, *3*, 252-262. https://doi.org/10.4236/cs.2012.33035

[7] Fazljoo, S. A., Aliabad, A. D., & Amiri, E. (2023). A novel air core electromagnetic fault current limiter with rotational motion. *IET Electric Power Applications*, *17*(6), 855-866. https://doi.org/10.1049/elp2.12309

[8] Amini, M., Aliabad, A. D., & Amiri, E. (2021). Design and analysis of fault current limiter based on air core variable series reactor. *IEEE Access*, *9*, 166129-166136. https://doi.org/10.1109/ACCESS.2021.3134870

[9] Calixte, E., Yokomizu, Y., Shimizu, H., Matsumura, T., & Fujita, H. (2004). Reduction of rating required for circuit breakers by employing series-connected fault current limiters. *IEE Proceedings-Generation, Transmission and Distribution*, *151*(1), 36-42. https://doi.org/10.1049/ip-gtd:20040060

[10] Ahmed, M. M. R., Putrus, G. A., Ran, L., & Xiao, L. (2001, April). Harmonic analysis and improvement of a new solid-state fault current limiter. *2001 Rural Electric Power Conference. Little Rock.* https://doi.org/10.1109/REPCON.2001.949528

[11] Nurminen, K. (2008). *Thermal modeling and evaluation of harmonic effects on a dry-type air-core reactor.* Doctoral dissertation, Helsinki University of Technology, 118.

[12] Cui, J. B., Shu, B., Tian, B., Sun, Y. W., Wang, L. Z., Gao, Y. Q., Liu, L., Wei, Z.Q., Zhang, L. F., Zhu, X. H., Li, Q., Hong, H., Cao, J. B., Gong, W. Z. & Xin, Y. (2013). Safety considerations in the design, fabrication, testing, and operation of the DC bias coil of a saturated iron-core superconducting fault current limiter. *IEEE Transactions on Applied Superconductivity*, *23*(3), 5600704. https://doi.org/10.1109/TASC.2012.2235493

[13] Majka, M. & Kozak, J. (2016). Superconducting fault current limiter for the electric power system. *Acta Physica Polonica A*, *130*(2), 581-584. https://doi.org/10.12693/APhysPolA.130.581

[14] Song, W., Pei, X., Xi, J., & Zeng, X. (2020). A novel helical superconducting fault current limiter for electric propulsion aircraft. *IEEE Transactions on Transportation Electrification*, *7*(1), 276-286. https://doi.org/10.1109/TTE.2020.2998417

[15] Dao, V. Q., Lee, J., Kim, C. S., & Park, M. (2020). Conceptual design of a saturated iron-core superconducting fault current limiter for a DC power system. *IEEE Transactions on Applied Superconductivity*, *30*(4), 5600905. https://doi.org/10.1109/TASC.2020.2968532

[16] Moyzykh, M., Gorbunova, D., Ustyuzhanin, P., Sotnikov, D., Baburin, K., & Maklakov, A. ... & Vavilov, A. (2021). First Russian 220 kV superconducting fault current limiter (SFCL) for application in city grid. *IEEE Transactions on Applied Superconductivity*, *31*(5), 5601707. https://doi.org/10.1109/TASC.2021.3066324

[17] Lim, S. T., Lim, S. H., & Han, T. H. (2017). Analysis on operation characteristics and power burdens of the double quench trigger type SFCLs. *Progress in Superconductivity and Cryogenics*, *19*(2), 33-37. https://doi.org/10.9714/psac.2017.19.2.033

[18] Yuhan, Z., He, J., Pan, Y., Yin, X., Ding, C., Ning, S., & Li, H. L. (2013). Thermal analysis of air-core power reactors. *International Scholarly Research Notices: Mechanical Engineering*, *2013*(1), 865015. https://doi.org/10.1155/2013/865015

[19] Yuan, F., Wu, K., Yuan, Z., Liu, J., Ding, C., Wang, Y., & He, J. (2018, October). Thermal optimization for dry type air core reactor base on FEM. *21st International Conference on Electrical Machines and Systems (ICEMS).* https://doi.org/10.23919/ICEMS.2018.8549257

[20] Huang, J., Zhu, Z., Liang, Y., & Fan, D. (2022). Analysis of the fault characteristics of DC microgrid and research on the parameter selection of current-limiting reactor. *2022 China International Conference on Electricity Distribution (CICED)*. https://doi.org/10.1109/CICED56215.2022.9929242

[21] Zhu, Y. & Li, Y. (2022). Optimal configuration of smoothing reactors and current limiting reactors in LCC-MMC HVDC network. *2022 IEEE 5th International Electrical and Energy Conference (CIEEC).* https://doi.org/10.1109/CIEEC54735.2022.9846447

[22] Zhou, J., Wang, H., Chen, S., Tian, P., Zhang, L., & Zhang, C. (2023). A digital twin system for comprehensive and dynamic temperature rise sensing of current-limiting reactors. *2023 IEEE 4th China International Youth Conference on Electrical Engineering (CIYCEE).* https://doi.org/10.1109/CIYCEE59789.2023.10401484

[23] Shah, A. (2023). Impact of current limiting reactor on bulk power network - A case study. *2023 IEEE Texas Power and Energy Conference (TPEC).* https://doi.org/10.1109/TPEC56611.2023.10078670

[24] Xing, C., Xi, X., He, X., Liu, M., & Li, S. (2020). Research on configuration of current limiting reactor in multi-terminal HVDC transmission system. *16th IET International Conference on AC and DC Power Transmission (ACDC 2020).* https://doi.org/10.1049/icp.2020.0028

[25] Zichen, L., Gang, S., Jianwen, Z., Xu, C., Nengqiao, W., & Jie, H. (2020). Parameter optimization for current limiting reactor and fault current limiter in MMC-HVDC. *2020 5th International Conference on Power and Renewable Energy (ICPRE).* https://doi.org/10.1109/ICPRE51194.2020.9233124

[26] Guo, Y., Wang, X., Liu, H., Liu, D., Wang, S., & Cheng, Q. (2020). Magnetizing inrush current blocking method for shunt reactor with auxiliary winding system. *2020 IEEE 4th Conference on Energy Internet and Energy System Integration (EI2).* https://doi.org/10.1109/EI250167.2020.9346898

[27] Akin, F., Arikan, O., & Kucukaydin, B. (2023). FEM based air-core reactor modelling for series inductor of SPRFCL. *2023 International Conference on Engineering and Emerging Technologies (ICEET).* https://doi.org/10.1109/ICEET60227.2023.10525922

[28] Wang, G., Fan, C., & Wang, S. (2021). A DC line protection scheme based on transient energy ratio on both sides of current-limiting reactor. *10th Renewable Power Generation Conference (RPG 2021).* https://doi.org/10.1049/icp.2021.2320

[29] Li, B., Liao, K., Yang, J., & He, Z. (2021). An improved differential protection strategy of DC distribution network with current limiting reactor. *2021 IEEE 5th Conference on Energy Internet and Energy System Integration (EI2).* https://doi.org/10.1109/EI252483.2021.9713093

[30] Chitaliya, G. H. & Joshi, S. K. (2015). Determination of short circuit stresses in an air core reactor using finite element analysis. *International Journal of Engineering, Science and Technology*, *7*(3), 141-147. https://doi.org/10.4314/ijest.v7i3.17S

[31] Hurkala, M. (2013). *Noise analysis of high voltage capacitors and dry-type air-core reactors*. Doctoral dissertation, Aalto University, 155/2013.

[32] Hagh, M. T. & Abapour, M. (2009). Nonsuperconducting fault current limiter with controlling the magnitudes of fault currents. *IEEE Transactions on Power Electronics*, *24*(3), 613-619. https://doi.org/10.1109/TPEL.2008.2008421

[33] Chen, S., Li, P., Lehman, B., Ball, R., & de Palma, J. F. (2013, March). A new topology of bridge-type non-superconducting fault current limiter. *2013 Twenty-Eighth Annual IEEE Applied Power Electronics Conference and Exposition (APEC).* https://doi.org/10.1109/APEC.2013.6520491

[34] Nazari-Heris, M., Nourmohamadi, H., Abapour, M., & Sabahi, M. (2016). Multilevel nonsuperconducting fault current limiter: Analysis and practical feasibility. *IEEE Transactions on Power Electronics*, *32*(8), 6059-6068. https://doi.org/10.1109/TPEL.2016.2618915

[35] Nourmohamadi, H., Nazari-Heris, M., Sabahi, M., & Abapour, M. (2017). A novel structure for bridge-type fault current limiter: Capacitor-based nonsuperconducting FCL. *IEEE Transactions on Power Electronics*, *33*(4), 3044-3051. https://doi.org/10.1109/TPEL.2017.2710018

[36] Ayaz, M., Tasdemirci, E., Yuce, M., Mese, E., & Hergul, A. S. (2020). Comparative study on winding materials for wind turbine alternators. *Emerging Materials Research*, *9*(2), 360-365. https://doi.org/10.1680/jemmr.19.00029

[37] Tezcan, M. M. & Ayaz, M. (2023). Performance analysis of aluminium wound double fed induction generator for cost-efficient wind energy conversion systems. *Engineering Research Express*, *5*(4), 045037. https://doi.org/10.1088/2631-8695/ad061b

[38] Khan, A., Ayaz, A., Khan, F., & Ullah, W. (2023, October). Performance comparison and experimental analysis of three-phase induction motor with aluminium and copper winding.

2023 International Conference on Technology and Policy in Energy and Electric Power (ICT-PEP). https://doi.org/10.1109/ICT-PEP60152.2023.10351149
[39] Abdullah-Al-Imran, M., Sumon, M. M. H., & Shah, K. M. (2015). Computer aided design and comparative study of copper and aluminium conductor wound distribution transformer. *American Journal of Engineering Research*, *4*(2), 133-145.
[40] Olivares-Galván, J. C., De León, F., Georgilakis, P. S., & Escarela-Perez, R. (2010). Selection of copper against aluminium windings for distribution transformers. *IET Electric Power Applications*, *4*(6), 474-485. https://doi.org/10.1049/iet-epa.2009.0297
[41] Yang, J., Zhang, W., Zou, L., Wang, Y., Sun, Y., & Feng, Y. (2019). Research on distribution and shielding of spatial magnetic field of a DC air core smoothing reactor. *Energies*, *12*(5), 937. https://doi.org/10.3390/en12050937
[42] Salinas, E., Atalaya, J., Hamnerius, Y., Solano, C. J., Gonzales, D., Contreras, C., ... & Rezinkina, M. (2007). A new technique for reducing extremely low frequency magnetic field emissions affecting large building structures. *The Environmentalist*, *27*(4), 571-576. https://doi.org/10.1007/s10669-007-9067-6
[43] Enohnyaket, M. & Ekman, J. (2009). Analysis of air-core reactors from DC to very high frequencies using PEEC models. *IEEE Transactions on Power Delivery*, *24*(2), 719-729. https://doi.org/10.1109/TPWRD.2008.2008421
[44] Zou, L., Gong, P., & Zhang, L. (2014). Small-scale experiment and model simplification of space magnetic fields around air-core reactors. *High Voltage Engineering*, *40*(6), 1675-1682.
[45] Sun, Y., Zou, L., Liu, Q., Dai, L., Zhang, L., & Zhao, T. (2021). Research on five-loop simplified scaling model for dry-type air-core reactors with inter-turn short circuit fault. *IEEE Access*, *9*, 163707-163715. https://doi.org/10.1109/ACCESS.2021.3118042
[46] See https://hilkar.com/tr/hcharmonikfiltrereaktorleri.html
[47] See https://www.lme.com/

Contact information:

Murat AYAZ, PhD, Associate Professor
(Corresponding author)
Kocaeli University,
Department of Electric and Energy,
41180, Kocaeli, Turkey
E-mail: murat.ayaz@kocaeli.edu.tr

Cüneyt CEYHAN, MSc
Kocaeli University, Turkey
E-mail: cuneytcyhn@gmail.com

Kadir YILMAZ, PhD, Assistant Professor
Kocaeli University,
Department of Energy Systems Engineering,
41050, Kocaeli, Turkey
E-mail: kayel@kocaeli.edu.tr

Yiğit KARABULUT, PhD
Manisa Celal Bayar University,
Department of Electrical & Electronic Engineering,
45030, Manisa, Turkey
E-mail: yigit.karabulut@cbu.edu.tr